



Initial insights from 2.5D hydraulic modeling of floods in Athabasca Valles, Mars

L. P. Keszthelyi,¹ R. P. Denlinger,² D. R. H. O'Connell,³ and D. M. Burr⁴

Received 24 August 2007; revised 3 October 2007; accepted 15 October 2007; published 14 November 2007.

[1] We present the first application of a 2.5D hydraulic model to catastrophic floods on Mars. This model simulates flow over complex topography and incorporates flood dynamics that could not be modeled in the earlier 1D models. We apply this model to Athabasca Valles, the youngest outflow channel on Mars, investigating previous bank-full discharge estimates and utilizing the interpolated Mars Orbiter Laser Altimeter elevation map as input. We confirm that the bank-full assumption does not fit the observed landforms. Instead, the channel appears more deeply incised near the source. Flow modeling also identifies several areas of special interest, including a dry cataract that coincides with a region of predicted high erosion. However, artifacts in the elevation data strongly impacted estimated stages and velocities in other areas. More extensive connection between the flood hydraulics and observed landforms awaits improved topographic data.

Citation: Keszthelyi, L. P., R. P. Denlinger, D. R. H. O'Connell, and D. M. Burr (2007), Initial insights from 2.5D hydraulic modeling of floods in Athabasca Valles, Mars, *Geophys. Res. Lett.*, 34, L21206, doi:10.1029/2007GL031776.

1. Introduction

[2] The role of past and present water is the current focus of the Mars Exploration Program. Athabasca Valles is widely considered to be the site of the most recent major aqueous floods on Mars [e.g., Tanaka and Scott, 1986; Edgett and Rice, 1995; Berman and Hartmann, 2002; Burr et al., 2002a; Plescia, 2003]. The channel system is located in the young equatorial lowlands of Elysium Planitia. The main branch is a 10 to 30 km wide, 300 km long flat-floored valley that tracks the northwestern side of a wrinkle ridge (Figure 1). The source of the channel is a segment of the Cerberus Fossae volcano-tectonic fissures, with two major loci of erosion visible in the northeastern corner of Figure 1. The average down-flow slope is only 0.05%. While it is currently impossible to precisely date the valley carving event, the floor can be dated using the density of impact craters. Though some model ages from impact crater size-frequency distributions suggest the floor is as young as a few million years [Hartmann and Berman, 2000; Burr et al., 2002a; Murray et al., 2005], an age of several tens of

millions of years is considered more likely [Plescia, 2003; McEwen et al., 2005]. In any case, the estimated dates are in the uppermost Amazonian Period.

[3] It is important to note that Athabasca Valles, and the Cerberus Palus basin that it empties into, are covered with platy-ridged material that new images have shown to be lava [Jaeger et al., 2007]. All the features of potential fluvial origin are draped by this vast lava flow. However, the thickness of this lava coating is only of order several meters, so the larger morphologic features in the channel are well preserved [Jaeger et al., 2007]. For example, a series of streamlined forms surrounds surviving impact craters and knobs of older highlands terrain. Also, distributary channels cut across the wrinkle ridge in several locations. Other flood-related landforms that have been reported include subaqueous dunes, longitudinal grooves, and layered sediments [Burr et al., 2002a, 2004; Burr, 2005]. These intra-channel features provide compelling evidence for fluid erosion within Athabasca Valles.

[4] The floods through Athabasca Valles have been previously modeled [Burr et al., 2002a, 2002b; Burr, 2003] using the 1-D HEC-RAS model from U.S. Army Corp of Engineers [Hydrologic Engineering Center, 2002]. A water flux of $1-2 \times 10^6 \text{ m}^3 \text{ s}^{-1}$ was estimated for a channel roughness corresponding to a Manning coefficient of $n = 0.04$ and assuming bank-full flow. However, there are a number of limitations of the HEC-RAS model and the assumptions used in the model runs. First, the earlier 1-D modeling cannot properly take into account the real (complex) topography that the flood interacted with [e.g., Burr, 2003]. Second, the use of the Manning coefficient derived from empirical terrestrial data has been shown to be inappropriate for Mars [Wilson et al., 2004]. Third, the assumption of bank-full flow is unlikely to be realistic [e.g., Leask et al., 2007]. Finally, the floodwaters may have carried enough sediment to affect the flow hydraulics [Komar, 1980] but only clean water has been modeled.

2. Description of the 2.5D Hydraulic Model

[5] The new numerical model allows substantially better simulation of floods. It was developed jointly by the U.S. Geological Survey and the U.S. Bureau of Reclamations over the past 5 years and constitutes the cutting edge in modeling terrestrial floods [Denlinger et al., 2002; O'Connell et al., 2002; Ostenaar et al., 2002; Wallick et al., 2003]. It solves the shallow-water flow equations over rugged three-dimensional (3D) terrain. For each increment in time, the flow calculation divides the domain of interest into finite volume cells, calculates the mass and momentum transfer between cells using Riemann methods, then sums the changes to update the cell variables and proceeds to the

¹Flagstaff Field Center, U.S. Geological Survey, Flagstaff, Arizona, USA.

²Cascades Volcano Observatory, U.S. Geological Survey, Vancouver, Washington, USA.

³William Lettis and Associates, Golden, Colorado, USA.

⁴Carl Sagan Center for the Study of Life in the Universe, Search for Extraterrestrial Intelligence Institute, Mountain View, California, USA.

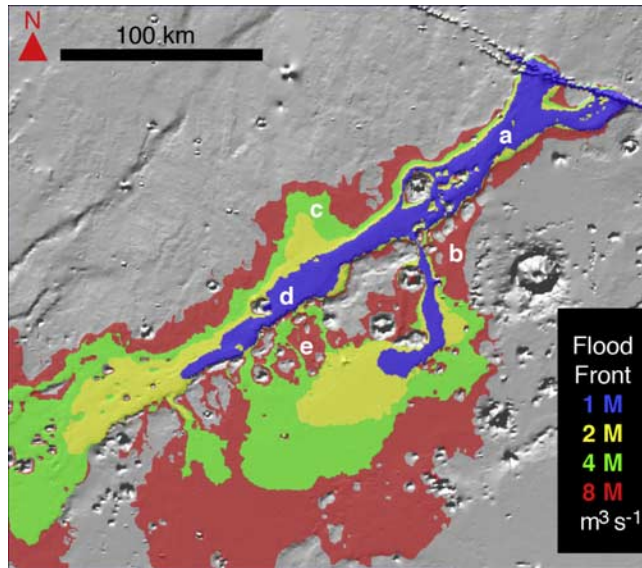


Figure 1. MOLA shaded relief view of Athabasca Valles with colors showing the extent of flood waters 30 hours into the simulation for discharges of 1, 2, 4, and 8 million $\text{m}^3 \text{s}^{-1}$. Letters a–e denote areas discussed in more detail in the text. Illumination is from the south.

next time increment. The method is naturally conservative, though care must be taken to properly conserve mass along the boundaries of the flow. A variety of fluids can be simulated, including water, mud, and lava. Changing gravitational acceleration to Mars was the only adjustment of the numerical code required before running the model for Athabasca Valles. We discuss some of the key improvements over previous models below.

2.1. Chezy C Friction Factor

[6] This form of the friction factor is based upon the scale of channel roughness and, unlike the Manning n , is not affected by changes in gravity and is consistent with measurements of fully turbulent flow and the ‘law of the wall’ [Pope, 2000]. For Athabasca Valles, the model was run with the same C values as used for the Pleistocene Missoula Floods which formed the Channeled Scabland in Montana, Idaho, Washington, and Oregon [Baker, 1973]. Those terrestrial floods cut through flood lavas covered by loess – a geologic setting analogous to Athabasca Valles [e.g., Jaeger et al., 2003].

2.2. Flow Over Complex Topography

[7] By explicitly accounting for non-hydrostatic flow within a shallow water model, using the method presented by Denlinger and Iverson [2004], the model accommodates flow transitions over drops, through chutes and pools, and across multiple current streams as flow occurs over rugged 3D terrain. Given an adequate topographic model, the effects of in-channel obstacles and distributary flow can be fully quantified. The accuracy of the model has been demonstrated for a variety of historical terrestrial floods [e.g., Denlinger et al., 2002; O’Connell et al., 2002; Ostenaar et al., 2002; Wallick et al., 2003].

2.3. Unsteady Flow

[8] The model calculates changes in flow with time, and has been used to demonstrate the effect of kinematic waves on routing of the Missoula Floods. The interaction of unsteady flood waves with 3D channel topography are likely to be responsible for many of the high-water marks inferred in Athabasca Valles.

2.4. Spatially Distributed Hydraulic Parameters

[9] The model outputs water surface elevation and velocity across the computational grid. Combining this information with surface roughness, we calculate stream power per unit area, a measure of the erosive potential of the flood. This information can be used to determine how erosion and/or deposition will change with time and location. The model output has been verified for a number of historical floods, where field data are compared with predictions of simulated flow over 3D model terrain [e.g., Denlinger et al., 2002; O’Connell et al., 2002; Ostenaar et al., 2002; Wallick et al., 2003].

2.5. Model Inputs

[10] The model inputs are (1) the topography over which the flood will travel, (2) the discharge rate, (3) the fluid properties, and (4) the location of the discharge. The best publicly available topographic data for Athabasca Valles is provided by the Mars Orbiter Laser Altimeter (MOLA) as a 128 pixels/degree digital terrain model (DTM). It is important to note that the cross-track distance between MOLA shots at this near-equatorial location can be >10 km. We found that some interpolation methods can improve the DTM in some areas, but they introduce other artifacts in other areas. In any case, no method can recreate features that were entirely missed by MOLA. After some experimentation, we decided to use the standard MOLA DTM.

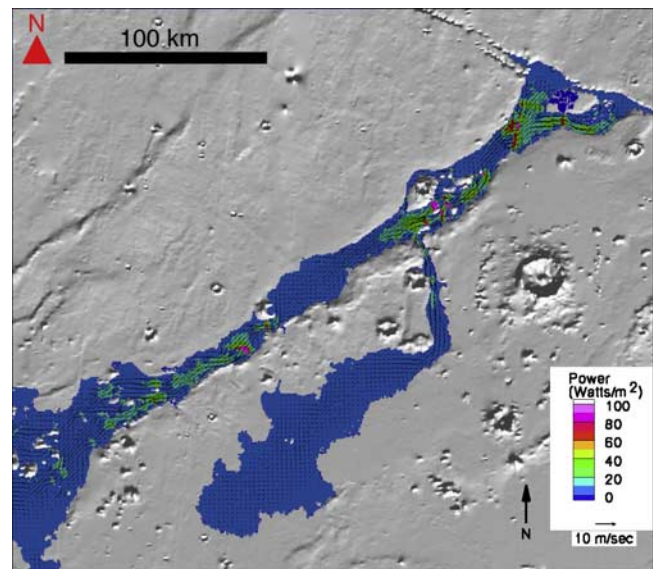


Figure 2. Plot of stream power and flow velocity 60 hours into the $1 \times 10^6 \text{ m}^3 \text{ s}^{-1}$ discharge run. Note how flow is accelerated through constrictions in the channel and the peaks in stream power at steps in the channel topography.

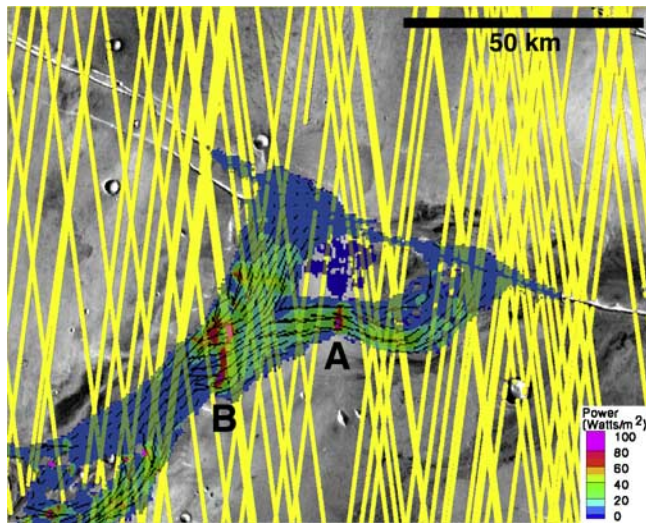


Figure 3. Model results from the near-source region. Stream power at 60 hours for the $1 \times 10^6 \text{ m}^3 \text{ s}^{-1}$ run overlaid on the THEMIS IR daytime mosaic. Yellow lines are MOLA tracks. There are two prominent areas with high stream power where enhanced erosion is predicted. The one labeled “A” is due to an interpolation artifact in the large gap between MOLA tracks. The other, labeled “B,” is found to correspond to a series of dry cataracts. Illumination is from the west.

[11] Typically the model is run to simulate dam-breaks and starts with a finite body of water that is catastrophically released. For Athabasca Valles, a fixed discharge was placed in the bottom of the Cerberus Fossae. As the fissures filled, the water then simply flowed out at the lowest low points along the rim. For this study, discharges of one, two, four, and eight million cubic meters per second were used, guided by the $1\text{--}2 \times 10^6 \text{ m}^3/\text{s}$ estimate from the earlier studies [e.g., Burr *et al.*, 2002a, 2002b, 2004; Burr, 2003]. We also only simulated clean water in this initial study.

3. Results

[12] The model output was visualized as a series of plots at select time steps showing water depth or stream power with flow velocity vectors overlain. Figure 2 is an example of one of these plots. In the model, it takes $\sim 1\text{--}10$ hours to fill the local segment of the Cerberus Fossae, as if the fissures had a volume of 36 km^3 . However, this is an overestimate because the interpolation in the MOLA DEM smooths the near-vertical walls of the Cerberus Fossae. Once it is flowing down the channel, the modeled flood behaves as expected. It enters distributary channels that cut over the wrinkle ridge and courses between the flood-formed features on the channel floor discussed by Burr *et al.* [2002a, 2002b].

[13] The previously published bank-full discharge estimates were derived from the upper reach of the main channel (labeled “a” in Figure 1). The simple geometry of this section was the most appropriate for the 1D HEC-RAS model [Burr, 2003]. The new simulations best fit the main topographic channel in this section with a discharge of

$1\text{--}2 \times 10^6 \text{ m}^3 \text{ s}^{-1}$. The match to the earlier HEC-RAS runs in this area is very encouraging. However, this range of discharge cannot reach some of the topographically higher distributary channels or streamlined forms. Those locations are filled when discharge is increased to $8 \times 10^6 \text{ m}^3 \text{ s}^{-1}$. This is clearest in the area labeled “b” in Figure 1, but is also evident on the north side of the section labeled “a”.

[14] Farther down the channel, a discharge of $2\text{--}4 \times 10^6 \text{ m}^3 \text{ s}^{-1}$ suffices to reach even the highest locations with visible water erosion. Interestingly, the $8 \times 10^6 \text{ m}^3 \text{ s}^{-1}$ run reaches far above any high water marks (e.g., the areas labeled “c” and “e” in Figure 1). Therefore we find a factor of ~ 2 decrease in the discharge required to run bank-full from the upper and lower reaches of Athabasca Valles. Some water must be lost during the roughly 1 day that it takes for the flow to traverse Athabasca Valles. However, neither evaporation nor infiltration can reasonably account for $4\text{--}6 \times 10^6 \text{ m}^3 \text{ s}^{-1}$ of water loss [e.g., Carr, 1996]. The more likely explanation is that the channel is more deeply incised near the source than in the middle and distal reaches. This modeling confirms earlier suspicions that the current channel was never filled with water.



Figure 4. Portion of MOC image S11-03177 showing a section of the series of dry cataracts found in the area labeled “B” in Figure 3. Image is centered at 9.86N, 156.69E and sinusoidally projected at 3.12 m/pixel. North is to the top, illumination is from the southwest, and overall flow was from east to west.

[15] The model also shows physically reasonable interactions with more complex topography (Figure 2). Water fills and stagnates within breached impact craters. The highest stream power is found where the flow is accelerated through constrictions concurrent with a step in topography. Superelevation is observed where the momentum of the flow carries water up the side of topographic obstacles. These results can be compared to the observed geomorphology. For example, the large apparently breached crater near the middle of the main channel (labeled “d” in Figure 1) would be an ideal location for slackwater sedimentation. The superelevation suggests that high-water marks will be higher on the stoss side than on the lee side of some obstacles. And high shear stress areas near the source are likely localities for potholes and other erosional features. Unfortunately, when we do examine the areas the model highlights, we find that many are artifacts in the MOLA DEM. For example, the breached crater near the center of the main channel is seen in image data to actually be a complete crater with no breach. The MOLA shot points missed the eastern rim, so the interpolated DEM shows a breach.

[16] Figure 3 highlights more interesting results from near the source area. One prominent location (labeled “A” in Figure 3) where the model shows high stream power falls in a wide gap between MOLA shot points. It turns out that the DEM interpolation algorithm inserted a step in the middle of this gap, which produces a fictional cataract in the channel floor. However, at the location labeled “B” the MOLA data is denser and the model indication of high stream power should be correct. Upon examination of the Mars Orbiter Camera (MOC) images of the area, we discovered a corresponding series of dry cataracts that have not been previously reported (Figure 4).

[17] We were particularly interested in determining the flow behavior around a concentration of streamlined forms between which the only reported subaqueous dunes on Mars can be found [Burr *et al.*, 2004]. However, the MOLA DEM does not resolve these kilometer-scale features and thus the estimated local flow not reliable. This same issue precludes our ability to confirm or refute superelevation around in-channel obstacles.

4. Conclusions

[18] The concurrence of the new 2.5D and the previous 1D modeling (where both are valid) confirms that the new model has been properly modified for Mars simulations. However, these discharges must be considered upper limits because they neglect that fact that the channel was incised by the flood and therefore the current topography probably never ran bank-full. Instead, it appears that the upper reaches of the channel system are much more deeply eroded than the distal parts. The flow model demonstrated its potential to predict the distribution of erosional and depositional landforms with the discovery of a dry cataract. However, in order to realize the full synergism between the modeling and the observed geomorphology, better topographic data is required. Improving the MOLA elevation model by incorporating Mars Express HRSC and Mars Reconnaissance Orbiter CTX stereo data should produce accurate DTMs at the appropriate scale for future studies.

Such future studies should include examining the effect of sediment in the water and time-varying discharge.

[19] **Acknowledgment.** This work was funded by the NASA Mars Data Analysis Program.

References

- Baker, V. R. (1973), Paleohydrology and sedimentology of Lake Missoula flooding in eastern Washington, *Spec. Pap. Geol. Soc.*, 144.
- Berman, D. C., and W. K. Hartmann (2002), Recent fluvial, volcanic, and tectonic activity on the Cerberus plains of Mars, *Icarus*, 159, 1–17.
- Burr, D. M. (2003), Hydraulic modelling of Athabasca Vallis, Mars, *Hydrol. Sci. J.*, 48, 655–664.
- Burr, D. M. (2005), Clustered streamlined forms in Athabasca Valles, Mars: Evidence for sediment deposition during floodwater ponding, *Geomorphology*, 69, 242–252.
- Burr, D. M., J. A. Grier, A. S. McEwen, and L. P. Keszthelyi (2002a), Repeated aqueous flooding from the Cerberus Fossae: Evidence for very recently extant, deep groundwater on Mars, *Icarus*, 159, 53–73.
- Burr, D. M., A. S. McEwen, and S. E. H. Sakimoto (2002b), Recent aqueous floods from the Cerberus Fossae, Mars, *Geophys. Res. Lett.*, 29(1), 1013, doi:10.1029/2001GL013345.
- Burr, D. M., P. A. Carling, R. A. Beyer, and N. Lancaster (2004), Flood-formed dunes in Athabasca Valles, Mars: Morphology, modeling, and implications, *Icarus*, 171, 68–83.
- Carr, M. H. (1996), *Water on Mars*, 229 pp., Oxford Univ. Press, Oxford, U. K.
- Denlinger, R. P., and R. M. Iverson (2004), Granular avalanches across irregular three-dimensional terrain: 1. Theory and computation, *J. Geophys. Res.*, 109, F01014, doi:10.1029/2003JF000085.
- Denlinger, R. P., D. R. H. O’Connell, and P. K. House (2002), Robust determination of stage and discharge: An example from an extreme flood on the Verde River, Arizona, in *Ancient Floods, Modern Hazards: Principles and Applications of Paleoflood Hydrology*, *Water Sci. Appl. Ser.*, vol. 5, edited by P. K. House *et al.*, pp. 127–146, AGU, Washington, D. C.
- Edgett, K. S., and J. W. Rice (1995), Very young volcanic, lacustrine, and fluvial features of the Cerberus and Elysium basin region, Mars: Where to send the 1999 Mars Surveyor Lander, *Lunar Planet. Sci. Conf.*, 26, 357–358.
- Hartmann, W. K., and D. C. Berman (2000), Elysium Planitia lava flows: Crater count chronology and geological implications, *J. Geophys. Res.*, 105, 15,011–15,026.
- Hydrologic Engineering Center (2002), HEC-RAS hydraulic reference manual, version 3.1, 350 pp., U.S. Army Corps of Eng. Hydrol. Eng. Cent., Davis, Calif.
- Jaeger, W. L., L. P. Keszthelyi, D. M. Burr, A. S. McEwen, V. R. Baker, H. Miyamoto, and R. A. Beyer (2003), Ring dike structures in the Channeled Scabland as analogs for circular features in Athabasca Valles, Mars, *Lunar Planet. Sci. Conf.*, 34, Abstract 2045.
- Jaeger, W. L., L. P. Keszthelyi, A. S. McEwen, C. M. Dundas, and P. S. Russell (2007), Athabasca Valles, Mars: A lava-draped channel system, *Science*, 317, 1709–1711.
- Komar, P. D. (1980), Modes of sediment transport in channelized water flows with ramifications to the erosion of the Martian outflow channels, *Icarus*, 42, 317–329.
- Leask, H. J., L. Wilson, and K. L. Mitchell (2007), Formation of Mangala Valles outflow channel, Mars: Morphological development and water discharge and duration estimates, *J. Geophys. Res.*, 112, E08003, doi:10.1029/2006JE002851.
- McEwen, A. S., B. S. Preblich, E. P. Turtle, N. A. Artemieva, M. P. Golombek, M. Hurst, R. L. Kirk, D. M. Burr, and P. R. Christensen (2005), The rayed crater Zunil and interpretations of small impact craters on Mars, *Icarus*, 176, 351–381.
- Murray, J. B., *et al.* (2005), Evidence from the Mars Express High Resolution Stereo Camera for a frozen sea close to Mars’ equator, *Nature*, 434, 256–352.
- O’Connell, D. R. H., D. A. Ostenaar, D. R. Levish, and R. E. Klinger (2002), Bayesian flood frequency analysis with paleohydrologic bound data, *Water Resour. Res.*, 38(5), 1058, doi:10.1029/2000WR000028.
- Ostenaar, D. A., D. R. H. O’Connell, R. A. Walters, and R. J. Creed (2002), Holocene paleoflood hydrology of the Big Lost River, western Idaho Engineering and Environmental Laboratory, Idaho, *Spec. Pap. Geol. Soc. Am.*, 353, 91–110.
- Plescia, J. B. (2003), Cerberus Fossae, Elysium, Mars: A source for lava and water, *Icarus*, 164, 79–95.
- Pope, S. B. (2000), *Turbulent Flows*, 806 pp., Cambridge Univ. Press, New York.

- Tanaka, K. L., and D. H. Scott (1986), The youngest channel system on Mars, *Lunar Planet. Sci. Conf.*, 17, 865–866.
- Wallick, J. R., R. Denlinger, S. Lancaster, and J. Bolte (2003), Assessing the role of floods, land conversion and bank materials in determining channel change along the Willamette River, *Eos Trans. AGU*, 84(46), Fall. Meet. Suppl., Abstract H42E-1121.
- Wilson, L., G. J. Ghatan, J. W. Head III, and K. L. Mitchell (2004), Mars outflow channels: A reappraisal of the estimation of water flow velocities from water depths, regional slopes, and channel floor properties, *J. Geophys. Res.*, 109, E09003, doi:10.1029/2004JE002281.
-
- D. M. Burr, Carl Sagan Center for the Study of Life in the Universe, SETI Institute, 515 N. Whisman Road, Mountain View, CA 94043-2172, USA.
- R. P. Denlinger, Cascades Volcano Observatory, U.S. Geological Survey, 1300 SE Cardinal Court, Building 10, Suite 100, Vancouver, WA 98683-9589, USA.
- L. P. Keszthelyi, Flagstaff Field Center, U.S. Geological Survey, 2255 N. Gemini Drive, Flagstaff, AZ 86001, USA. (laz@usgs.gov)
- D. R. H. O'Connell, William Lettis and Associates, 433 Park Point Drive, Golden, CO 80401, USA.